

# Effect of Al alloying on the Hall-Petch strengthening and AE in compressed Mg-Li-Al alloys before and after HPT processing

S. Kúdela<sup>1\*</sup>, A. Pawełek<sup>2</sup>, Z. Ranachowski<sup>3</sup>, A. Piątkowski<sup>2</sup>, S. Kúdela Jr.<sup>1</sup>, P. Ranachowski<sup>3</sup>

<sup>1</sup>*Institute of Materials and Machine Mechanics, Slovak Academy of Sciences,  
Račianska 75, 831 02 Bratislava, Slovak Republic*

<sup>2</sup>*Aleksander Krupkowski Institute of Metallurgy and Materials Science, Polish Academy of Sciences,  
Reymonta 25, 30-059 Kraków, Poland*

<sup>3</sup>*Institute of Fundamental Technological Research, Polish Academy of Sciences,  
Świętokrzyska 21, 00-049 Warszawa, Poland*

Received 21 December 2010, received in revised form 30 March 2011, accepted 19 April 2011

## Abstract

The paper deals with the effect of Al content in two-phase Mg-10Li- $x$ Al ( $x = 0, 1, 5$ ) alloys on their straining behaviour before and after severe plastic deformation by high pressure torsion. Both coarse-grained and ultrafine-grained alloys were compression strained in channel-die device with simultaneous acoustic emission monitoring. It has been observed that Hall-Petch strengthening in ultra-fine grained alloys superposes with the strengthening resulting from Al alloying (solution hardening, particulate strengthening). Superposition of these strengthening mechanisms becomes stronger with increase in Al content, presumably due to enhanced grain refining effect.

**Key words:** Mg-Li-Al alloys, grain refinement, high pressure torsion, acoustic emission, Hall-Petch strengthening

## 1. Introduction

Alloying of magnesium with lithium significantly reduces its density and markedly improves the cold formability. Nevertheless, Mg-Li based alloys possess relatively low strength, especially those with high Li content. To reach the strength-ductility compromise, two-phase Mg-Li alloys (4–11 wt.% Li) are preferred in which stiffer hcp  $\alpha$ -phase is dispersed within ductile bcc  $\beta$ -matrix [1]. In these alloys, hcp  $\alpha$ -phase is Mg(Li) solid solution while bcc  $\beta$ -phase is Li(Mg) one without forming intermetallics [2]. Because of similar atomic radii no significant solute strengthening takes place in binary Mg-Li alloys. Adding of aluminium causes additional strengthening either by Al solute or by the precipitation of metastable MgAlLi<sub>2</sub> and/or stable AlLi phases [3]. This makes Mg-Li alloys more suitable for engineering applications.

Application of severe plastic deformation (SPD) on two-phase based Mg-Li alloys refines both  $\alpha$  and  $\beta$  constituents down to submicron sizes thus initiat-

ing considerable Hall-Petch strengthening [4, 5]. It is worthy to note that in two-phase Mg-Li based alloys the Hall-Petch strengthening may be frustrated by very high Li diffusivity in  $\beta$ -phase that initiates the Coble type creep even at the room temperature [6]. A question arises how the Hall-Petch strengthening superposes with other strengthening mechanisms (solid solutions precipitation) operating in ultrafine-grained two-phase Mg-Li-Al alloys. Present paper deals with this topic.

Three two-phase Mg-Li alloys differing in their hardening mechanisms were selected for current experiments: Mg10Li (no hardening), Mg10Li1Al (solution hardening) and Mg10Li5Al (solution and precipitation hardening). These alloys were prepared by melting & casting followed with high pressure torsion (HPT) to create the sub-microcrystalline structure. HPT is considered the most powerful SPD technique for producing exceptionally small grain sizes [7]. Both coarse- and ultrafine-grained alloys were compression strained in channel-die device with simultaneous acoustic emis-

\*Corresponding author: tel. +421 2 49268229; e-mail address: [ummskuds@savba.sk](mailto:ummskuds@savba.sk)

sion (AE) monitoring. Main intention of this work is to examine the interplay between the strengthening resulting from Al alloying and the Hall-Petch strengthening in HPT processed Mg-Li-Al alloys.

## 2. Experimental

### 2.1. Alloys preparation

The alloys with nominal compositions of Mg-10wt.%Li, Mg-10wt.%Li-1wt.%Al and Mg-10wt.%Li-5wt.%Al were prepared by the melting of pure magnesium, lithium and aluminium (purities of 99.9 %, 99.0 % and 99.9 %, respectively) followed by casting into cold low-alloyed steel mould ( $40 \times 40 \times 20 \text{ mm}^3$ ). Both melting and casting operations were conducted in the same chamber under argon pressure of 0.5 MPa after previous evacuation. The actual alloy compositions as determined by wet chemical analysis were Mg-9.88wt.%Li, Mg-9.92wt.%Li-1.03wt.%Al and Mg-9.74wt.%Li-4.74wt.%Al. The alloys prepared were naturally aged during long-term storage (more than 40 days) at ambient temperature.

### 2.2. High pressure torsion

HPT was conducted in constrained version at the room temperature in which the disc-shaped sample was inserted into the cavity between two anvils and torsionally strained by 1–3 rotations of the upper anvil under the compression of 3 GPa. After  $N$  rotations, for a disc sample with the radius of  $R$  and the height of  $l$ , the dilatational strain  $\gamma = (2\pi RN)/l$  and the equivalent strain  $\varepsilon_N = \gamma/1.73$  have been reached [7]. The discs before HPT were 10 mm in diameter and 2 mm in thickness.

### 2.3. Channel-die compression

The channel-die test is a plane strain test in which the specimen is compressed by the punch while the lateral spreading is blocked by two walls so that the sample can extend only along a single direction thus creating biaxial stress state. Compression in channel-die set was performed in testing machine INSTRON-3382 under the traverse velocity of  $0.05 \text{ mm min}^{-1}$  wherein external loading  $F$  was continuously recorded. The channel-die block was made of quenched steel having the distance of 10 mm between the side walls. The size of disc samples tested (10 mm in diameter) was nearly the same as the walls distance. Channel-die assembly greatly facilitates the transduction of AE signal from deformed sample to recording apparatus which enables to detect very weak AE signals emitted by ultrafine-grained structures. This was the main reason why the channel-die version was used

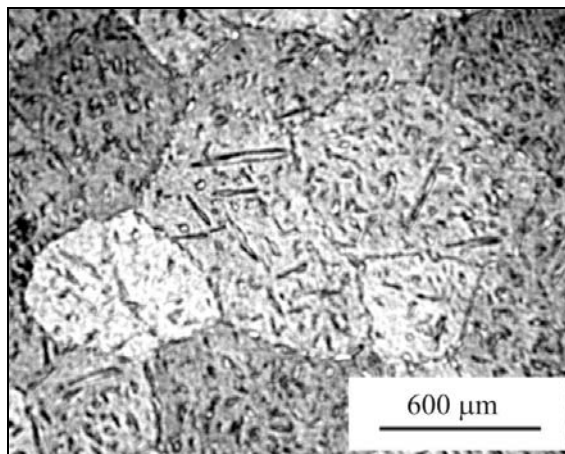


Fig. 1. Optical micrograph of as-cast Mg10Li alloy. Etching agent: 2 % HCl in water-free iso-propanol.

for straining experiments. The samples tested were of identical geometry to compare their loading-strain responses.

### 2.4. Acoustic emission

The disc samples were inserted into channel-die block on a thick parallelepiped ceramics rod serving as a waveguide for AE signals. The samples were covered with teflon foil to eliminate the friction effects. Total amplification of the AE analyzer was 70 dB and the sampling frequency was 44.1 kilosamples per second. Each AE signal registered contained 300 MB data of digital samples. The files recorded were converted using the numerical program to obtain the plot AE event rates versus time.

## 3. Results and discussion

### 3.1. Coarse grained alloys

Equilibrium Mg-Li phase diagram predicts that Mg-10wt.%Li alloy has a two-phase structure  $\alpha + \beta$  in which  $\alpha$ -MgLi (hcp) is dispersed in  $\beta$ -MgLi (bcc) [8]. Such a dual structure is formed during solidification of respective Mg-Li liquid (L) wherein  $\alpha$  constituent precipitates from  $\beta$  matrix by the Widmanstätten type solidification  $L \rightarrow \beta \rightarrow \alpha + \beta$  as the temperature decreases. Accordingly, current Mg10Li alloy consists of polycrystalline  $\beta$  matrix with fairly large grains (500–600  $\mu\text{m}$ ) inside which about one order of magnitude single-crystalline  $\alpha$  phase is uniformly dispersed (Fig. 1). Volume fraction of  $\alpha$  phase (about 12 %) was determined by the linear intercept method.

AE of channel-die strained diphasic Mg10Li alloy can be roughly considered the sum of AE of  $\alpha$  and  $\beta$  constituents. Earlier AE inspections of single phase

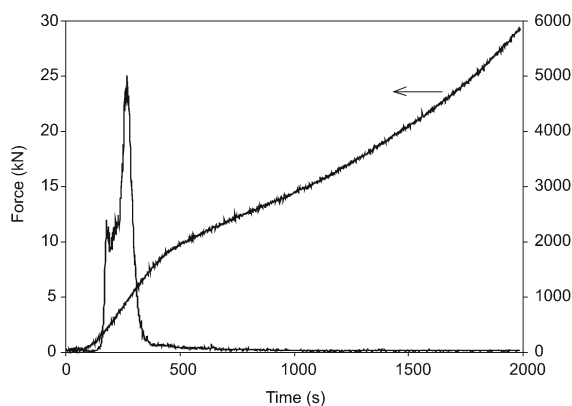


Fig. 2. AE events rate and force versus time during channel-die compression of as-cast Mg10Li.

$\alpha$ -Mg4Li and  $\beta$ -Mg12Li alloys have revealed that AE response of  $\alpha$ -Mg4Li was about 3–4 orders of magnitude higher than that of  $\beta$ -Mg12Li [9]. Strong continuous AE signal in the vicinity of yield point falling rapidly down to the base level emitted from  $\alpha$ -Mg4Li can be related to massive dislocation slip on pyramidal planes of hcp phase activated by the decrease in cell parameters ratio  $c/a$  due to Li alloying [10]. On the other hand, weak AE bursts produced by  $\beta$ -Mg12Li appeared irregularly during whole straining period exhibiting significant maximum around the yield point are indicative of dislocation climb promoted by extremely fast diffusion of Li in bcc structure [11]. These results will be used below to elucidate AE behaviour of present Mg-Li and Mg-Li-Al alloys.

Dramatically different AE activities of  $\alpha$  and  $\beta$  components suggest that resultant AE of diphasic Mg10Li alloy reflect mainly the contribution of  $\alpha$  phase despite its small volume fraction. Accordingly, channel-die strained Mg10Li alloy produces continuous AE patterns qualitatively similar to that of single phase  $\alpha$ -Mg4Li. After reaching its maximum AE falls rapidly down being kept on very low level over the whole post-yielding period (Fig. 2). As already mentioned, such an AE response can be ascribed to crystallographic slip in  $\alpha$  phase mainly under participation of non-basal dislocations [12].

Low-temperature equilibrium Mg-Li-Al phase diagram suggests that Mg10Li1Al has a two-phase  $\alpha + \beta$  structure while Mg10Li5Al should consist of three phases, namely  $\alpha$ ,  $\beta$  and AlLi [13]. Natural ageing of Mg-Li-Al alloys leads to the precipitation of coherent MgLiAl<sub>2</sub> that transforms to incoherent AlLi particles during long-term room-temperature storage [14]. It is remarkable that fine particles AlLi (50–100 nm) precipitate only in  $\beta$  region mainly around  $\alpha/\beta$  boundaries while no precipitation occurred in  $\alpha$ -phase [15, 16].

Rapid drop in AE activity of Mg10Li1Al can be

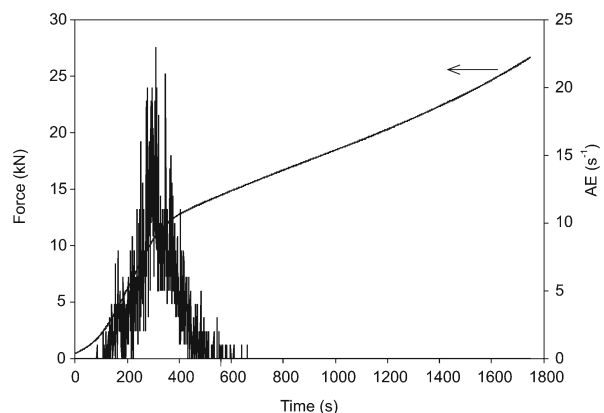


Fig. 3. AE events rate and force versus time during channel-die compression of as-cast Mg10Li1Al.

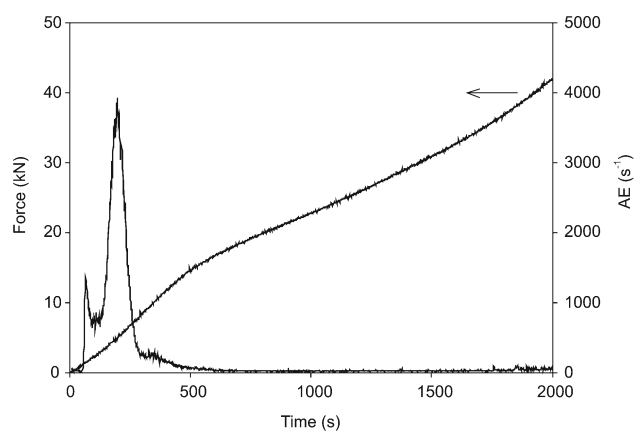


Fig. 4. AE events rate and force versus time during channel-die compression of as-cast Mg10Li5Al.

ascribed to enhanced resistance of dislocation slip in hcp  $\alpha$ -phase due to dissolved Al atoms. AE record of Mg10Li1Al remains still continuous exhibiting minor bursts that are likely generated by inhomogeneous plastic flow due to the interaction of mobile dislocations with Al solute (Fig. 3). Twinning as other possible source of AE bursts has not been evidenced by microstructural observations.

In contrast, strong continuous AE signal of Mg10-Li5Al alloy, resembling that of Mg10Li, suggests that no hardening occurs in  $\alpha$ -phase despite high nominal Al content (Fig. 4). Reason for this rather surprising observation is unclear at present. It may be tentatively explained with earlier precipitation of AlLi from supersaturated  $\beta$ -matrix during cooling thus leaving too little Al amount for the strengthening of  $\alpha$ -phase. Note that similar AE features appeared also during channel-die compression of two-phase Mg8Li $x$ Al alloys ( $x$  varied between 0 and 5) [9].

The relation between AE and mechanical responses of current Mg10Li based alloys is not straightforward

because AE matches practically only the yielding of  $\alpha$ -phase while the macroscopic yielding depends on both  $\alpha$  and  $\beta$  constituents. Moreover, because of quite low volume fraction of  $\alpha$ -phase, the macroscopic strength seems to be governed mainly with  $\beta$  phase. The load-time curves demonstrate that Al adding to Mg10Li causes considerable alloy strengthening (Figs. 2–4). When taking the departure from the linear course as the indication of the yielding onset, it is seen that the loadings at which Mg10Li, Mg10Li1Al and Mg10Li5Al start to yield (8, 10 and 13 kN, respectively) increase persistently with Al content. This observation is consistent with the yielding data reported for two-phase Mg-Li-Al alloys in the literature [2, 3]. Present AE records indicate that in Mg10Li1Al significant hardening of  $\alpha$ -phase takes place due to Al alloying, while in Mg10Li5Al no hardening of  $\alpha$ -phase is recognizable despite high nominal Al content. This suggests that macroscopic strengthening in Mg10Li5Al is entirely at the expense of  $\beta$  constituent (solid solution, precipitation).

AE records in Figs. 2–4 also show that onsets of macroscopic yielding of alloys tested are asynchronous with the maxima of AE signals appearing in the pre-yielding period. This phenomenon can be explained with the microplasticity resulting from complex multi-axial loading taking place during channel-die straining [17].

### 3.2. Ultrafine grained alloys

Application of HPT on current Mg-Li and Mg-Li-Al alloys resulted in great refinement of their structures (Fig. 5). TEM images show that their structure consists of nearly equiaxed  $\alpha$  and  $\beta$  grains with the size of several hundreds nanometers, i.e. they are by 2 and 3 orders of magnitude smaller than in as-cast state (Figs. 6a,b). Hence,  $\beta$ -grains have been refined much faster than  $\alpha$ -phase which agrees with obser-

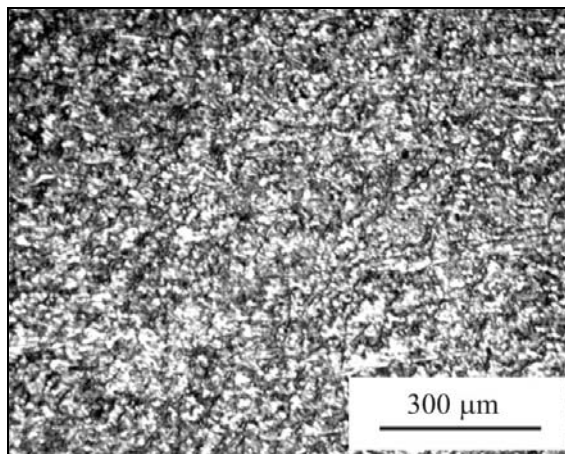


Fig. 5. The refining effect in Mg10Li alloy after HPT procedure. Optical micrograph (no etching).

vations reported by other authors [5]. It is also seen that Al alloyed samples after HPT exhibit considerably finer structure than Mg10Li: while Mg10Li after HPT has the mean grain size 400–500 nm (Fig. 6a), that in Mg10Li5Al is about 100 nm (Fig. 6b). Favourable effect of alloying on the grain refinement during SPD is generally explained with decreasing recovery rate in solid solution alloys, either through reduction in dislocation mobility [18] or lowering in stacking fault energy [19]. These observations imply that generation of ultra-fine structure during SPD is governed mainly with the coalescence of subgrains while the condensation of dislocation tangles and formation of cells in early recovery stage are of lesser relevance.

Mechanical behaviour of ultrafine grained metals ( $1 \mu\text{m} > d > 0.1 \mu\text{m}$ ) is usually interpreted in terms of the core-mantle model dividing the grains into a grain interior (core) and a grain-boundary region (mantle) [20]. According to this concept, mantle (thickness of 10–100 nm) produces the starter dislocations that

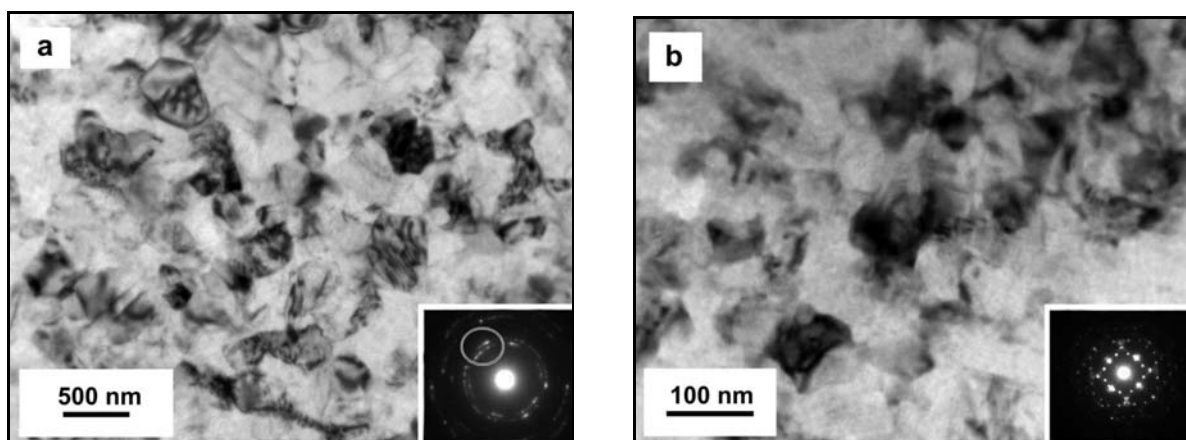


Fig. 6. TEM images of UFG structures after 3 HPT rotations – peripheral parts of disc samples: (a) Mg10Li, (b) Mg10Li5Al.

Table 1. Loads at the yielding onset and sums of AE events recorded during channel-die compression of both as-cast samples and HPT processed samples

Alloy material	Load of yielding onset (kN)	Sum of AE events, $\times 10^3$
Mg10Li, as-cast	8	979
Mg10Li, after HPT (3 rotations)	12	33
Mg10Li1Al, as-cast	10	9.7
Mg10Li1Al, after HPT (2 rotations)	16	1.4
Mg10Li1Al, after HPT (3 rotations)	16	0.8
Mg10Li5Al, as-cast	13	914
Mg10Li5Al, after HPT (3 rotations)	22	124

cross-slip and multiply upon emission inside the grains thus creating a work-hardened zone. Consequently, the dislocation pile-up is formed that reduces free paths of mobile dislocations and constrains their movement which leads to rapid decrease in AE activity. Moreover, the dislocation motion loses its collective behaviour so the grains are deformed by successive motion of individual dislocations as manifested by burst-like AE patterns [21, 22].

There are collected in Table 1 the sums of recorded AE events and the yielding onsets of channel-die compressed alloys before and after HPT. It is seen that ultrafine-grained samples are markedly stronger than those coarse-grained. In both cases the strength tends to increase with increase in Al content. Accordingly, the yielding onset of as-cast alloys increases along the series Mg10Li – Mg10Li1Al – Mg10Li5Al by  $\sim 62\%$  (8–10–13 kN), while corresponding increase after HPT operation is  $\sim 83\%$  (12–16–22 kN). This suggests that Hall-Petch strengthening after HPT rises more rapidly with Al alloying. Apart from other possible reasons, it may be connected with the above mentioned favourable effect of Al alloying on the grain refinement.

The solution strengthening in nanostructured alloys generally operates in the same way as in conventional coarse-grained alloys [23]. Thus, in ultra-fine grained Mg10Li1Al it may be expected the superposition of Hall-Petch strengthening and the hardening due to Al solute. On the other hand, the superposition of Hall-Petch strengthening and precipitation hardening in Mg10Li5Al is hardly expectable because the grain sizes after HPT (about 100 nm) are nearly comparable with the size of incoherent AlLi precipitates (50–100 nm). In this case the Orowan type mechanism operating in single grains through formation of dislocation loops around particles cannot be effective. The particulate composite strengthening is known to cause only relatively small increase in the yielding stress. Therefore, the only relevant strengthening in ultrafine grained Mg10Li5Al seems to be connected with the grain refinement of  $\beta$ -phase combined with Al solute hardening, while the strengthening with AlLi particles is of minor significance.

AE patterns of Mg10Li alloy after three HPT ro-

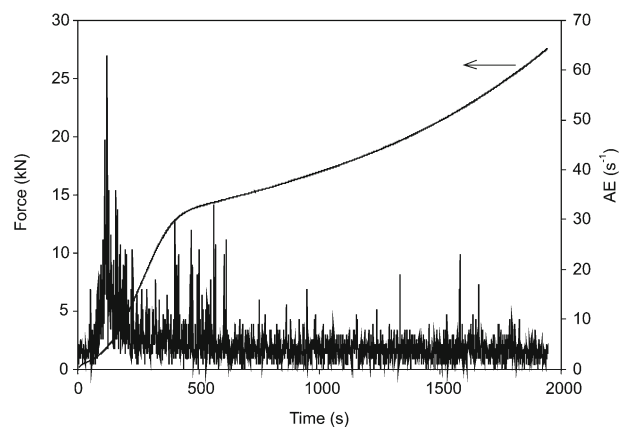


Fig. 7. AE events rate and force versus time during compression test of Mg10Li alloy after HPT (3 rotations).

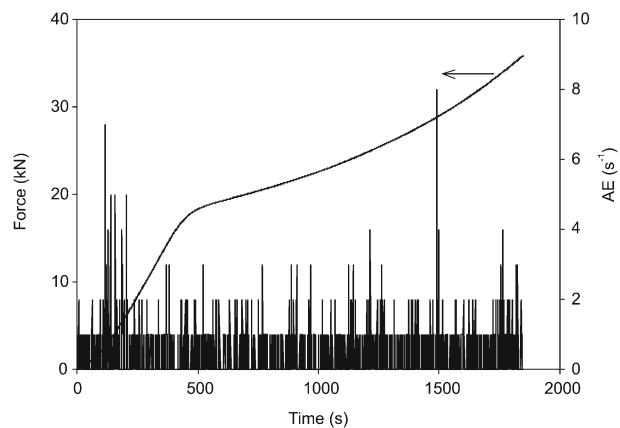


Fig. 8. AE events rate and force versus time during compression test of Mg10Li1Al after HPT (2 rotations).

tations are essentially of continuous type exhibiting pronounced bursts with the maximum in pre-yielding stage (Fig. 7). This suggests that dislocation slip in  $\alpha$ -phase is strongly restricted, apparently due to rapid size reduction. Smaller AE bursts appearing during entire post-yielding period may indicate the sliding and/or decohesion at  $\alpha/\beta$  interfaces.

Figures 8 and 9 show AE records of Mg10Li1Al

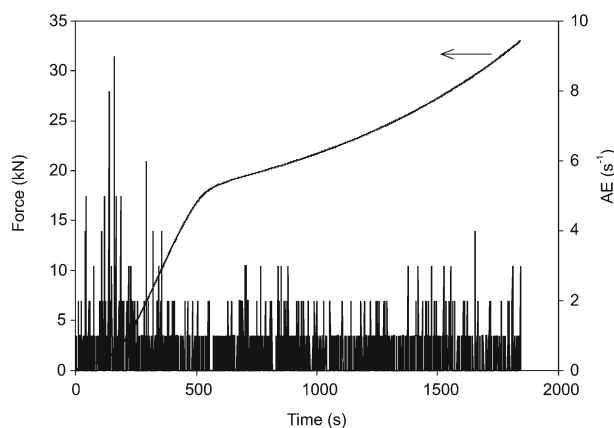


Fig. 9. AE events rate and force versus time during compression test of Mg10Li1Al after HPT (3 rotations).

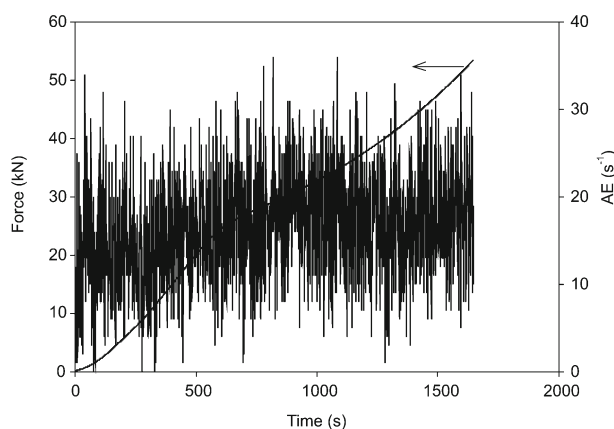


Fig. 10. AE events rate and force versus time during compression test of Mg10Li5Al after HPT (3 rotations).

alloy after two and three HPT rotations, respectively, indicating nearly comparable very small burst-like AE maxima in the pre-yielding period followed with AE bursts slightly over the base level. Such an exceedingly low AE activity is attributable to the hindering of dislocation slip due to the coupled effect of dissolved Al atoms and grain size refinement. Negligible AE bursts in the post-yielding period may be ascribed to the slip and/or decohesion at  $\alpha/\beta$ .

AE count rate for Mg10Li5Al alloy after 3-fold HPT is shown in Fig. 10. Unlike the coarse-grained Mg10Li5Al, monotonous burst-like AE counts appear over entire straining period reaching the level of about  $30 \text{ s}^{-1}$ . Extensive refinement of  $\alpha$ -phase down to  $\sim 100 \text{ nm}$  imposes strong obstruction on the dislocation slip so that continuous AE fully disappears. Decohesion of  $\alpha$ -particles and/or incoherent AlLi precipitates occurring in  $\beta$  matrix may operate as possible sources of AE bursts, similar to those observed typically in particle strengthened metallic composites [24] and/or ageing hardened metallic alloys [25].

#### 4. Concluding remarks

The present results suggest that Hall-Petch strengthening in Mg10Li, Mg10Li1Al and Mg10Li5Al alloys after HPT is roughly additional to the strengthening from Al alloying (solid solution, precipitation). In other words, the higher initial strength of coarse grained alloys, the higher strength of respective ultra-fine grained ones. Moreover, significant progressivity in Hall-Petch strengthening with increase in Al content has been observed. The refinement degree by HPT is significantly promoted by Al alloying wherein the final grain sizes vary roughly between 100 and 500 nm. Remarkable strengthening in HPT processed Mg10Li1Al may be attributed to the coupled effect of solution hardening and grain refinement while the strengthening in HPT processed Mg10Li5Al can be ascribed mainly to the grain refinement and hardening with Al solute at the solubility limit. It is believed that the strength level of alloys studied is mainly governed with the strength of matrix  $\beta$ -phase as the volume fraction of  $\alpha$ -phase is quite small (12 vol.%). AE provides useful additional information on the relation between the structure refinement and the deformation behaviour, even though it matches mainly the mechanical response of  $\alpha$ -phase. Strongly suppressed dislocation slip in HPT processed samples is displayed by rapid drop in AE activity which more or less copies the trends of the size reduction of  $\alpha$ -phase. Weak AE bursts observed in Mg10Li5Al after HPT may be ascribed to the friction of  $\alpha$ -grains and/or AlLi intermetallics with  $\beta$  matrix.

#### Acknowledgements

There are acknowledged the Grant Agency VEGA of the Slovak Republic (Project 2/0196/11) as well as Agency for Science and Research of the Slovak Republic (Project VMSP-P-0036-07) for supporting this work. The study was also supported by the Polish Ministry of Science and High Education (Research Project No N N507 598038).

#### References

- [1] HAFERKAMP, H.—JASCHIK, C.—JUCHMANN, P.—KAESE, V.—NIEMEYER, M.—TAI, P.: *Materiálovývedenie a Werkstofftechnik*, 32, 2001, p. 25. [doi:10.1002/1521-4052\(200101\)32:1<25::AID-MAWE25>3.3.CO;2-A](https://doi.org/10.1002/1521-4052(200101)32:1<25::AID-MAWE25>3.3.CO;2-A)
- [2] DRITS, M. E.—YELKIN, F. M.—GUREV, I. I.—BONDAREV, B. I.—TROKHOVA, V. F.—SERGIEVSKAYA, A. D.—OSOKINA, T. N.: *Magnesium-Lithium Alloys*. Moscow, Metallurgija 1980 (in Russian).
- [3] SCHEMME, K.: *Development of Super-Light Magnesium Materials*. VDI Fortschritt-Berichte Nr. 293/Reihe 5, Düsseldorf, VDI-Verlag 1993 (in German).

- [4] KAMADO, S.—ASHIE, T.—OHSHIMA, Y.—KOJIMA, Y.: *Materials Science Forum*, 350-351, 2000, p. 55. [doi:10.4028/www.scientific.net/MSF.350-351.55](https://doi.org/10.4028/www.scientific.net/MSF.350-351.55)
- [5] LIU, T.—ZHANG, W.—WU, S. D.—JIANG, C. B.—LI, S. X.—XU, Y. B.: *Materials Science & Engineering*, 360A, 2003, p. 345.
- [6] KIM, W. J.: *Scripta Materialia*, 61, 2009, p. 652. [doi:10.1016/j.scriptamat.2009.06.001](https://doi.org/10.1016/j.scriptamat.2009.06.001)
- [7] ZHILYAEV, A. P.—LANGDON, T. G.: *Progress in Materials Science*, 53, 2008, p. 893. [doi:10.1016/j.pmatsci.2008.03.002](https://doi.org/10.1016/j.pmatsci.2008.03.002)
- [8] NAYEB-HASHEMI, A. A.—CLARK, J. B.—PELTON, A. B.: *Bulletin of Alloy Phase Diagrams*, 5, 1984, p. 365. [doi:10.1007/BF02872951](https://doi.org/10.1007/BF02872951)
- [9] PAWELEK, A.—PIATKOWSKI, A.—KÚDELA, S.—JASIENSKI, Z.—LITWORA, A.: *Molecular and Quantum Acoustics*, 23, 2002, p. 351.
- [10] AGNEW, S. R.—HORTON, J. A.—YOO, M. H.: *Metallurgical & Materials Transactions*, 33A, 2002, p. 851.
- [11] WEI, X. W.—ZU, X. T.—ZHOU, W. L.: *Materials Science & Technology*, 22, 2006, p. 730. [doi:10.1179/174328406X86083](https://doi.org/10.1179/174328406X86083)
- [12] KAMADO, S.—KOJIMA, Y.: *Metallurgical Science & Technology*, 16, 1998, p. 45.
- [13] LEVINSON, D. W.—McPHERSON, D.: *J. Transactions of the ASM*, 48, 1956, p. 689.
- [14] SANSCHAGRIN, A.—TREMBLAY, R.—ANGERS, R.—DUBE, D.: *Materials Science & Engineering*, 220A, 1996, p. 69.
- [15] KIM, D. H.—HAN, Y. S.—LEE, H. I.—CANTOR, B.: *Scripta Metallurgica et Materialia*, 31, 1994, p. 819. [doi:10.1016/0956-716X\(94\)90485-5](https://doi.org/10.1016/0956-716X(94)90485-5)
- [16] KIM, Y. W.—KIM, D. H.—LEE, H. I.—HONG, C. P.: *Scripta Materialia*, 38, 1998, p. 923. [doi:10.1016/S1359-6462\(97\)00573-3](https://doi.org/10.1016/S1359-6462(97)00573-3)
- [17] YUDIN, A. A.—IVANOV, V. I.: *Strength of Metals*, 17, 1985, p. 842. [doi:10.1007/BF01528739](https://doi.org/10.1007/BF01528739)
- [18] IWANASHI, Y.—HORITA, Z.—NEMOTO, M.—LANGDON, T. G.: *Metallurgical & Materials Transactions*, 29A, 1998, p. 2503.
- [19] ZHAO, Y. H.—LIAO, X. Z.—ZHU, Y. T.—HORITA, Z.—LANGDON, T. G.: *Materials Science & Engineering*, 410-411A, 2005, p. 188.
- [20] MEYERS, M. A.—MISHRA, A.—BENSON, D. J.: *Progress in Materials Science*, 51, 2006, p. 427. [doi:10.1016/j.pmatsci.2005.08.003](https://doi.org/10.1016/j.pmatsci.2005.08.003)
- [21] VINOGRADOV, A.: *Scripta Materialia*, 39, 1998, p. 797.
- [22] LOUCHET, F.—WEISS, J.—RICHETON, T.: *Physical Review Letters*, 97, 2006, p. 075504-1. [doi:10.1103/PhysRevLett.97.075504](https://doi.org/10.1103/PhysRevLett.97.075504) PMID:17026245
- [23] SCATTERGOOD, R. O.—KOCH, C. C.—MURTY, K. L.—BRENNER, D.: *Materials Science & Engineering*, 493A, 2008, p. 3.
- [24] REES, D. W. A.: *Composites*, 29A, 1998, p. 171.
- [25] RUSBRIDGE, K. L.—SCRUBY, C. B.—WADLEY, H. N. G.: *Materials Science & Engineering*, 59, 1983, p. 151. [doi:10.1016/0025-5416\(83\)90164-7](https://doi.org/10.1016/0025-5416(83)90164-7)